Interference between Compton Scattering and X-Ray Parametric Down-Conversion

Kenji Tamasaku* and Tetsuya Ishikawa

RIKEN SPring-8 Center, 1-1-1 Koto, Sayo-cho, Sayo-gun, Hyogo 679-5148 Japan

(Received 15 December 2006; published 14 June 2007)

Parametric down-conversion of x rays into extreme ultraviolet and accompanying nonlinear x-ray diffraction were investigated both theoretically and experimentally. The theory predicted a rocking curve having a Lorentzian signal peak; however, the experiments revealed a peak followed by an unexpected dip. Together with the scattering angle dependence of the signal, the experimental results implied a possibility of interference between the Compton scattering and the parametric down-conversion. The similarity to the Fano effect is discussed.

DOI: 10.1103/PhysRevLett.98.244801 PACS numbers: 41.50.+h, 42.25.Fx, 42.65.Lm

Theoretical and experimental knowledge of nonlinear x-ray optics is quite limited [1], although the linear process is understood well. The situation is considerably different from the visible region, where nonlinear optics is indispensable. The reason may be the pessimistically small efficiency of the nonlinear process in the x-ray region; e.g., the second order nonlinear susceptibility is about 10 orders of magnitude smaller than that in the visible region. However, forthcoming x-ray free-electron lasers (XFEL) [2] should make a breakthrough in the field of nonlinear x-ray optics because of the very high peak electric field strength. Furthermore, quantum optics could be extended to the x-ray region. Before the emergence of XFEL, we have to deepen our understanding of nonlinear x-ray optics as much as possible.

Some of the nonlinear processes are observable and may be measurable with sufficient precision for investigation of the nonlinear x-ray optics. One of the most interesting and basic nonlinear process accessible at present is parametric down-conversion of x rays, especially, into the extreme ultraviolet (EUV), which we will refer as $X \rightarrow X + \mathrm{EUV}$ parametric down-conversion hereafter. The process is interesting by itself as nonlinear x-ray optics, while it has important applications. It was predicted that the nonlinear susceptibility for covalently bonded materials would be determined by the valence-electron charge density [3], which is difficult to estimate from the total charge density measured by the linear process. In spite of the importance, there has been only one experimental report [4]. The reported result with large uncertainty is insufficient for verification of the prediction. Further experimental evidences are desirable to understand the process and to apply it for structural analysis.

In the $X \rightarrow X + \mathrm{EUV}$ parametric down-conversion, one x-ray photon, called the pump, converted into two photons in the x-ray region, called the signal, and in the EUV region, called the idler. It requires conservation of energy and momentum before and after the conversion. The refractive index is close to unity in the x-ray region and cannot be used for momentum conservation (phase matching). A quite different method using reciprocal lattice vectors was proposed in the x-ray region [5], so that the parametric down-conversion is observed as a result of nonlinear x-ray diffraction. However, theoretical and experimental understanding of the nonlinear x-ray diffraction is insufficient as well as the $X \rightarrow X + \mathrm{EUV}$ parametric down-conversion.

In this Letter, we will give a brief summary of our theory of nonlinear x-ray diffraction. We will present the first synchrotron radiation (SR) measurements of the $X \rightarrow X + \mathrm{EUV}$ parametric down-conversion process and reveal unknown features of the nonlinear diffraction.

The wave equations of parametric down-conversion for the signal and the idler waves are written as [6],

$$\nabla \times \nabla \times \mathcal{E}_s - (1 + 4\pi\chi_s)K_s^2\mathcal{E}_s = 4\pi K_s^2\chi^{(2)}\mathcal{E}_p\mathcal{E}_i^* \qquad (1a)$$

$$\nabla \times \nabla \times \mathcal{E}_i - (1 + 4\pi\chi_i)K_i^2\mathcal{E}_i = 4\pi K_i^2\chi^{(2)}\mathcal{E}_p\mathcal{E}_s^*. \qquad (1b)$$

Here $\mathcal{E}$ is the electric field strength, χ is the linear susceptibility, $\chi^{(2)}$ is the second order nonlinear susceptibility, and K is the wave vector in the vacuum. The subscripts p, s, and i denote the physical quantities for the pump, the signal, and the idler waves, respectively. We apply the slowly varying amplitude approximation for simplicity. Solving (1) with the similar technique to the dynamical theory of x-ray diffraction [7] gave the identical result.

Now we limit our discussion to the diffraction geometry in the "symmetric Bragg" case. The signal wave is supposed to emerge from the incident surface of the pump wave, and the surface normal is to be parallel to the reciprocal lattice vector, Q, used for phase matching. Ignoring the second derivative of amplitude and depletion and absorption of the pump wave reduces (1),

$$\frac{\partial A_s}{\partial \xi} = \kappa_s A_i^* e^{i\Delta k \xi} \qquad (2a)$$

$$\frac{\partial A_i^*}{\partial \xi} = \kappa_i^* A_s e^{-i\Delta k \xi} + \mu_i A_i^*. \qquad (2b)$$

Here A is the amplitude and μ is the amplitude attenuation coefficient. The ξ axis is taken towards the propagation direction of the signal wave as shown in Fig. 1(a). The idler wave is assumed to propagate towards the negative ξ direction. We introduce quantities, $\kappa_s = 2\pi i K_s^2 \chi_Q^{(2)} A_p / |k_s|$ and $\kappa_i^* = -2\pi i K_i^2 \chi_Q^{(2)*} A_p^* / |k_i|$, where k is the wave vector in the medium for $A_p = 0$, and $\chi_Q^{(2)}$ is the Qth Fourier coefficient of $\chi^{(2)}$. The wave vector mismatch, Δk, is given by $\Delta k = k_p + Q - k_s - k_i$. The general solution may be given as $A_s(\xi) = (C \sinh g\xi + D \cosh g\xi) \exp(i\Delta k \xi/2)$ and $A_i^*(\xi) = (F \sinh g\xi + G \cosh g\xi) \exp(-i\Delta k \xi/2)$. The constants C, D, F, and G are to be determined under appropriate boundary conditions.

Nontrivial solution of (2) exists when $g = \pm\sqrt{\kappa^2 - \Delta k^2/4}$ for $\mu_i = 0$. Here, $\kappa^2 = \kappa_s \kappa_i^* = 4\pi^2 K_s^2 K_i^2 |\chi_Q^{(2)}|^2 |A_p|^2 / k_s k_i$. The roots for $\mu_i = 0$ indicate that there is no gain except for the exact phase matching, i.e., $\Delta k = 0$, because κ^2 is quite small as will be estimated later. When there is finite absorption for the idler wave, the gain is available over much wider range of Δk. The roots for $\mu_i \neq 0$ are given by

$$g_+ = \frac{\kappa^2 \mu_i}{\Delta k^2 + \mu_i^2} + i\left[\frac{\Delta k}{2} - \frac{\kappa^2 \Delta k}{\Delta k^2 + \mu_i^2}\right] \tag{3a}$$

$$g_- = -\mu_i - \frac{\kappa^2 \mu_i}{\Delta k^2 + \mu_i^2} - i\left[\frac{\Delta k}{2} - \frac{\kappa^2 \Delta k}{\Delta k^2 + \mu_i^2}\right], \tag{3b}$$

where we assumed $\mu_i \gg \kappa$ and ignored the higher order terms than κ^4. The first root with positive real part, (3a), has gain. The gain is found to be a Lorentzian with respect to Δk and have a width of $2\mu_i$. On the other hand, the second root, (3b), suffers strong absorption.

The experiment was performed at the RIKEN SR physics beam line (BL19LXU) at SPring-8 to use the brightest x rays from the 27-m in-vacuum undulator [8]. The energy of the pump wave was $E_p = 11.0$ keV. The photon flux (density) of the pump wave was 9.3×10^{11} photons/s (1.9×10^{14} photons/s/mm^2). To make clear the nature of nonlinear diffraction, the incidence was plane wave without any focusing. The energy of the signal wave was selected to be $E_s = 11.0 + \Delta E$ keV by a bent crystal analyzer with the Ge 220 reflection [Fig. 1(b)]. The energy resolution of the analyzer was measured to be 2.2 eV. A solid angle of $\Delta\Omega_s = 1.4 \times 10^{-5}$ sr was monitored for the signal wave. The idler wave cannot be measured due to strong absorption in the EUV region.

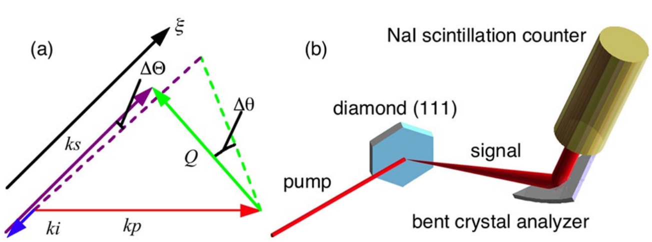

FIG. 1 (color online). (a) The phase-matching geometry used in the theoretical calculation and the experiment. Dashed lines indicate the geometry for $E_i = 0$, i.e., the Bragg diffraction. (b) Schematic view of the experimental setup.

We used a high quality synthetic type IIa diamond crystal with the (111) surface as the nonlinear medium. The rocking curve of the linear diffraction agreed well with the theoretical curve due to very low defect density [9], suitable for investigation of the nonlinear diffraction. Diamonds have another advantage that the ratio between the core- and the valence-electron binding energies is large enough [3]. The 111 reciprocal lattice vector was used for the phase matching. We used a particular geometry for phase matching, where k_s was antiparallel to k_i [Fig. 1(a)]. The geometry makes the signal wave emitted into a relatively large solid angle with a narrow spectrum [4] and was convenient to raise the signal-to-noise ratio with the analyzer.

The 111 Fourier coefficient of the nonlinear susceptibility was estimated to be $|\chi_{111}^{(2)}| = 2.8 \times 10^{-16}$ esu for $E_s = 10.9$ keV and $E_i = 100$ eV [3]. Here we calculated the linear structure factor of the bond charge to be $F_{111}^V = 4.5$, approximating it with spherical Gaussian [10,11]. The peak electric field strength of the incidence was estimated to be 6.7 esu. From these values, we estimated $\kappa^2 = 2.1 \times 10^{-30}$ Å^{-2}, which was sufficiently small, as assumed during the theoretical consideration.

Figure 2(a) shows the energy spectrum of scattered x rays from the nonlinear crystal. The glancing angle of the pump wave and the scattering angle of the signal wave were set to $\Delta\theta_0 = 1.92°$ and $\Delta\Theta_0 = 0.275°$ [Fig. 1(a)], which fulfilled the phase-matching condition,

$$K_p + Q = n_i K_i + K_s, \tag{4}$$

at $E_s = 10.9$ keV. Here n was the refractive index. These angles, $\Delta\theta$ and $\Delta\Theta$, were measured from the Bragg angle, θ_B, and the scattering angle, $2\theta_B$, respectively. A broad Compton peak was observed below the elastic peak at $\Delta E = 0$ eV (11.0 keV). The signal peak was found at the predicted energy of $\Delta E = -100$ eV on the lower energy tail of the Compton peak.

To verify the origin of the peak, the phase-matching condition was changed by $\Delta\theta$. The energy of peak shifted by -20 eV when $\Delta\theta$ changed from 1.92° to 2.32° [Fig. 2(b)]. The wave number shift of the signal wave related to $\Delta\theta$ by a simple geometrical relation,

$$\frac{dK_s}{d\Delta\theta} = -\frac{|K_p||Q| \cos\theta_B}{(n_i + 1)[(n_i + 1)|K_s| - n_i|K_p|]}. \tag{5}$$

The energy shift due to a rotation of 0.40° was calculated to be -21 eV by (5), in good agreement with the observation. Furthermore the azimuthal dependence was checked to eliminate the possibility of accidental linear diffraction. The peak was unchanged as expected for the parametric down-conversion, even when the crystal was rotated by 20° within the (111) net plane.

We tried to fit the tail of Compton spectrum with the Klein-Nishina formula to extract the signal wave contribution. However, the ambiguity of fitting was so significant

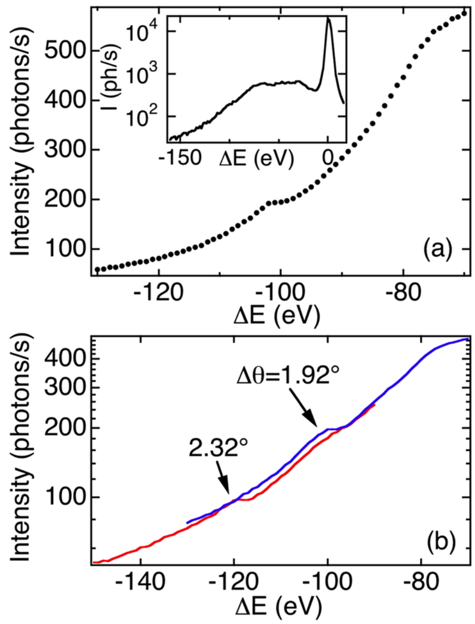

FIG. 2 (color online). (a) Energy spectrum measured under the phase-matching condition at $E_s = 10.9$ keV. Inset shows the spectrum in a wider energy range. (b) The energy spectra measured under the phase-matching conditions at $\Delta\theta_0 = 1.92°$ and 2.32°.

due to fine structures, e.g., a large bump at $\Delta E \sim -75$ eV [Fig. 2(b)].

Rocking curve.—Figure 3 shows the rocking curve of the nonlinear diffraction measured at $\Delta E = -100$ eV. In case of the nonlinear diffraction, measuring the rocking curve corresponded to changing E_s, or, equivalently, to scanning $\Delta k = (\Delta\theta - \Delta\theta_0)|Q| \cos\theta_B$ [Fig. 1(a)]. Note that the energy of the analyzer was fixed. The signal structure of the rocking curve was more pronounced than the energy spectrum. The background was fitted well with a polynomial. The overall angular dependence was attributed mainly to self-absorption of the signal wave by the nonlinear crystal.

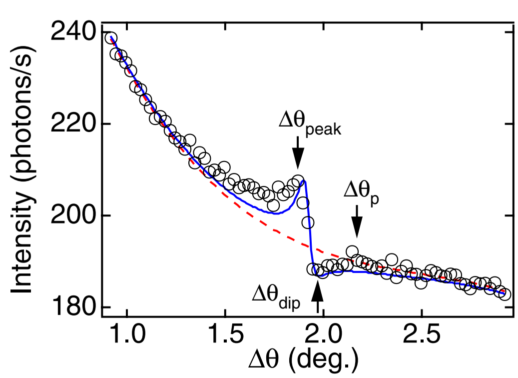

FIG. 3 (color online). The rocking curve of the nonlinear diffraction measured at $\Delta E = -100$ eV. Dashed line is polynomial fitting to the Compton background. The solid line is fitting with (7).

The most striking feature was that the rocking curve had not only the signal peak but also a dip. The peak was understandable as the phase-matched signal wave. However, the existence of the dip contradicted the above theory predicting a Lorentzian peak. The dip indicated decrease of the background Compton scattering. At the dip, the parametric down-conversion *did* occur, but interfered with the Compton scattering.

Width of rocking curve.—The signal structure extended over a wider angular range, $\sim 0.6°$. If the width had been determined by the well-known phase-matching condition, $|\Delta kl| < 1$ [6], the angular range should be 0.15 μrad. According to the discussion of (3a), the angular width of the present theory, W, was given by

$$W = 2\mu_i/|Q| \cos\theta_B. \tag{6}$$

The strong absorption for the idler wave, i.e., $\mu_i = 4.3\ \mu\text{m}^{-1}$ at 100 eV, relaxed the phase-matching condition greatly, and gave a wider width, $W = 0.017°$. However, it was still narrower than the observation.

Scattering angle dependence.—Figure 4 shows the $\Delta\Theta$ dependence of the signal intensity at $\Delta E = -100$ eV measured at fixed detuning angles at the peak $\Delta\theta_{\text{peak}}$ and the dip $\Delta\theta_{\text{dip}}$ on the rocking curve (Fig. 3). The signal wave was observed around the calculated scattering angle, $\Delta\Theta = 0.275°$, within an angular range of 0.4°, because phase matching at $E_s = 10.9$ keV was not satisfied at the scattering angles outside the observed peak.

An interesting feature was that the angular range for the dip was also limited. If the parametric down-conversion had reduced the available incident flux for the Compton scattering, the background should be suppressed over the whole scattering directions. This observation was considered to be another evidence of the interference of the parametric down-conversion with the Compton scattering. We performed a similar measurement at $\Delta\theta_p$ on the rocking curve (Fig. 3). There found no sign of the parametric down-conversion at $\Delta\theta_p$. The overall $\Delta\Theta$ dependence was due to the self-absorption.

Now we consider the underlying process which caused the asymmetric and the wider rocking curve and interference with the Compton scattering. We considered that these unexpected observations might be characteristics of Fano effect [12]. In this picture, the continuum excitation was supposed to be the Compton scattering, and the discrete excitation was the phase-matched $X \rightarrow X + \text{EUV}$ parametric down-conversion. It is an open question whether such a picture is valid or not. The most controversial point may be whether the ‘‘configuration interaction’’ exists [12].

We would like to analyze the rocking curve under the above scenario. We fitted the rocking curve with the formula,

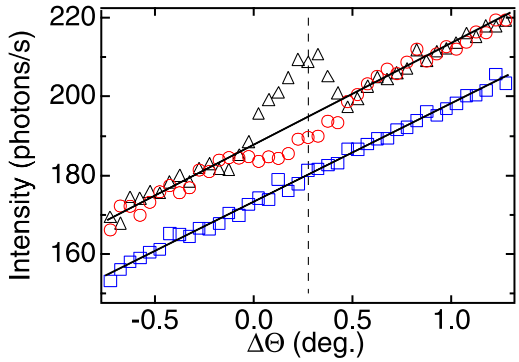

FIG. 4 (color online). Scattering angle dependence of the signal intensity at $\Delta E = -100$ eV at three characteristic glancing angles, $\Delta\theta_{\text{peak}}$ (△), $\Delta\theta_{\text{dip}}$ (○), and $\Delta\theta_p$ (□). Vertical line at 0.275° is the theoretical scattering angle under the exact phase-matching condition at $E_s = 10.9$ keV. The data for $\Delta\theta_p$ were shifted vertically by -10 for clarity. Solid lines are provided as a guide to the eye.

$$I = I_b + I_0\left[\frac{(q+\epsilon)^2}{1+\epsilon^2} - 1\right], \tag{7}$$

where I_b was the Compton background, I_0 was a constant, q was the asymmetric parameter, and ϵ was given by $\epsilon = (dK_s/d\Delta\theta)(\Delta\theta - \Delta\theta_0)/(\Gamma/2)$, where the derivative was given by (5) and Γ was the linewidth of the discrete excitation. We used the same polynomial as before, which was determined by using the data shown in Fig. 4. The parameters for best fitting to the rocking curve (Fig. 3) were $I = 5.5$, $q = 1.6$, and $\Gamma = 17.2\ \mu\text{m}^{-1}$.

The rocking curve was reproduced relatively well by (7). The Fano effect gave a wider signal structure with a narrower linewidth. We note that Γ was twice as large as the width predicted by (3a). The finite solid angle for the signal wave detection would broaden the width, especially, in the lower angle side of the rocking curve. The reason why there remained finite intensity at the dip, i.e., at the antiresonance ($\epsilon = -q$), was considered that only a small portion of the electrons contributing to the Compton scattering related to the parametric conversion. The effective number of electrons for the Compton scattering was estimated to be 27.5 per unit cell [13], which was much larger than $F_{111}^V = 4.5$ for the parametric conversion.

At present, lack of theoretical understanding of the nonlinear diffraction did not allow us to determine the true intensity of the signal, and, hence, to judge whether the valence-electron charge density was related or not. However, it may be interesting to compare the theory and the experiment. We estimated the signal intensity, using additional informations such as the measured efficiency of the analyzer (including air attenuation), 61.2%, and the effective crystal thickness, $l = 2.56$ mm. The intensity under the present experimental condition was calculated to be 61 photons/s [3]. When we regarded the difference of the intensity, 22 ± 1.4 photons/s, between the peak and the dip as the signal intensity (Fig. 3), it was 3 times smaller than the theoretical estimation.

In summary, the rocking curve of the nonlinear diffraction for $X \rightarrow X + \text{EUV}$ parametric down-conversion was not Lorentzian which was deduced by solving the wave equations. The existence of the peak and the dip, confined in the certain range of scattering angle, was considered as a result of interference between the Compton scattering and the $X \rightarrow X + \text{EUV}$ parametric down-conversion, though the microscopic mechanism is an open question. We pointed out the similarity of the observations to the Fano effect and showed that the effect reproduced the rocking curve relatively well. To understand the effect, further experimental and theoretical investigations are desired.

We would like to note that a backward parametric oscillator [14] may be possible with nonlinear diffraction at $\theta_B = \pi/2$ using nonlinear crystals in the x-ray region or nonlinear photonic crystals in the visible region.

We are grateful to Dr. Yoshihito Tanaka of RIKEN for helpful discussions.

*Present address: Department of Precision Science and Technology, Graduate School of Engineering, Osaka University, 2-1 Yamada-oka, Suita, Osaka 565-0871 Japan.
tamasaku@spring8.or.jp

[1] P. L. Shkolnikov and A. E. Kaplan, Inst. Phys. Conf. Ser. **151**, 512 (1996).
[2] SCSS X-FEL Conceptual Design Report, RIKEN Harima Institute, 2005; Stanford Linear Accelerator Center Report No. SLAC-R-521, 1998; Deutches Elektronen Synchrotron Report No. DESY97-048, edited by R. Brinkmann, G. Materlik, J. Rossback, and A. Wagner, 1997.
[3] I. Freund, Chem. Phys. Lett. **12**, 583 (1972).
[4] H. Danino and I. Freund, Phys. Rev. Lett. **46**, 1127 (1981).
[5] I. Freund and B. F. Levine, Phys. Rev. Lett. **23**, 854 (1969).
[6] R. Boyd, *Nonlinear Optics* (Academic, New York, 2003), Chap. 2.
[7] A. Authier, *Dynamical Theory of X-Ray Diffraction* (Oxford University Press, Oxford, 2001).
[8] M. Yabashi *et al.*, Nucl. Instrum. Methods Phys. Res., Sect. A **467–468**, 678 (2001).
[9] K. Tamasaku, T. Ueda, D. Miwa, and T. Ishikawa, J. Phys. D: Appl. Phys. **38**, A61 (2005).
[10] I. Freund and B. Levine, Phys. Rev. Lett. **25**, 1241 (1970).
[11] B. Dawson, Proc. R. Soc. A **298**, 264 (1967).
[12] U. Fano, Phys. Rev. **124**, 1866 (1961).
[13] *International Tables for Crystallography* (Kluwer Academic Publishers, Dordrecht, 1999), Vol. C, Chap. 6.1.
[14] S. E. Harris, Appl. Phys. Lett. **9**, 114 (1966).